Human Factors and Ergonomics in Design, Vol. 210, 2026, 286–297
https://doi.org/10.54941/ahfe1007450

Thermal Illusion for Wearables: Effects of Vibrotactile Parameters and Placement on Thermal Masking and Comfort

Jiaqi Zheng[1], Wei Wang[1,2,3], Guanhua Sun[1], and Ruixiao Zheng[1]

[1] Hunan University, Changsha, 410082, China
[2] Lushan Lab, China
[3] Hunan Provincial Key Laboratory of Intelligent Human Factors Design, China

ABSTRACT

Within the increasing capability of computing and battery of handheld and wearable electronics, device heating has become a critical issue of user comfort and hardware usability. From Gate Control Theory, haptic stimulation may mitigate the thermal discomfort. Through two within-subjects experiments, we examined whether vibrotactile stimulation can attenuate contact-heat unpleasantness and whether placement on the upper limb provides the most actionable design guidance. Experiment 1 screened vibrotactile parameters using 7-point ratings and found an efficacy-tolerability trade-off: amplitude and duty cycle dominated perceived outcomes, whereas frequency had comparatively small effects. We therefore fixed frequency at 150 Hz and selected three candidate codes (221/231/232) spanning strong-effect to balanced profiles. Experiment 2 evaluated these candidates during individualized ramped heating (baseline vs. vibration) using window-locked metrics within 35–48 °C. Vibration generally reduced unpleasantness relative to baseline. Placement effects were most reliable in the mid-to-high window (L2; Friedman $\chi^2 = 7.87$, $p = 0.0195$), driven by robust forearm attenuation (Wilcoxon $p = 0.0054$, $dz \approx -0.73$). Vib-code differences were not stable at the group level, although some codes showed within-window reductions. Late-window results were treated as exploratory due to sparse sampling under conservative stop criteria.

Keywords: Thermo-tactile interaction, Vibrotactile stimulation, Thermal masking, Haptics, Hardware usability

INTRODUCTION

Within the growing capability of chipsets and battery, handheld and wearable electronics generate noticeable surface heat during use, raising both comfort and safety concerns for skin contact. Prior work on consumer devices has reported enclosure temperatures reaching the mid-45 °C range in realistic usage, a regime where perceived warmth can become distinctly uncomfortable depending on exposure duration and contact conditions (Zhang et al., 2017). Even when temperatures remain within guideline-relevant limits (e.g., ISO 13732 framing), subjective discomfort can be substantial; for example, a 42 °C surface held on the skin for tens of seconds can elicit high discomfort ratings (Zhang et al., 2017). These observations motivate

Received February 28, 2026; Revised April 4, 2026; Accepted April 20, 2026; Available online July 20, 2026

thermal management strategies that consider not only safety thresholds and engineering constraints, but also user-perceived thermal ergonomics by shaping the subjective experience of contact heating.

Traditional thermal management relies on engineering solutions (e.g., throttling power or adding heatsinks/fans), but these can conflict with device cost, size, and performance trade-offs (Zhang et al., 2017, 2016). As a complementary strategy from human factors perspective, other haptic stimulation such as vibrotactile has been explored as a perceptual means to mitigate thermal discomfort without materially lowering temperature (Singhal et al., 2017; Peiris et al., 2019). This rationale draws on Gate Control Theory: non-nociceptive tactile input can "close the gate" on pain signals by activating large-diameter afferents that inhibit nociceptive transmission in the spinal cord (Melzack and Wall, 1965; Mendell, 2014). Beyond peripheral gating, thermo-tactile interactions may also operate through attentional capture and multisensory integration—shifting the salience, interpretation, and moment-to-moment weighting of thermal inputs in perception (Villemure and Bushnell, 2002; Singhal et al., 2017). Together, these mechanisms support vibration as a low-power perceptual intervention for improving thermal comfort in interactive devices (Peiris et al., 2019; Singhal et al., 2017).

Despite growing evidence for vibrotactile attenuation of thermal discomfort, product-oriented guidance remains limited. Beyond the general existence of thermo-tactile interactions, sensory and pain research suggests that masking/analgesic effects are inherently spatial: the magnitude of modulation depends on where tactile input is delivered relative to the noxious thermal site, reflecting site-dependent receptor populations and neural weighting (e.g., thermo-tactile illusions and related paradigms) (Singhal et al., 2017; Craig and Bushnell, 1994; Green, 1977, 2004). Likewise, vibrotactile analgesia studies show that concurrent vibration can reduce heat pain, but typically evaluate a single placement and therefore provide limited evidence for how placement should be chosen to maximize mitigation (Lundeberg, 1984; Kakigi and Shibasaki, 1992; Roy et al., 2003). Consequently, vibration location remains an under-specified design variable in the context of thermal discomfort mitigation, even though actuator placement is often more actionable than changing enclosure temperature in a finalized product.

Empirically, stronger attenuation has often been reported when vibration is delivered adjacent to (or contralateral to) the heated site rather than directly on it (Yarnitsky et al., 1997; Casale and Hansson, 2022), suggesting that spatial configuration may materially shape efficacy. This is plausible given that vibrotactile sensitivity is strongly site-dependent: glabrous thenar/palm skin is highly vibration-sensitive, whereas hairy forearm skin is typically less so (Johansson and Vallbo, 1979). In addition, joint-adjacent regions such as the wrist/elbow can act as perceptual anchors that improve localization along the forearm (Cholewiak and Collins, 2003). Accordingly, this study compared three placements—the thenar eminence, volar wrist, and proximal volar forearm—to test how location shapes vibration-based attenuation of thermal discomfort, and whether location is a stronger determinant than vibration code under concurrent heating.

To capture the progression from warmth to discomfort and near-pain, we used an individualized ramped heating protocol (L1–L3) with continuous real-time thermal discomfort ratings, enabling threshold-anchored tests of vibrotactile modulation during contact heating. This ramped design better reflects progressive device warming than a fixed-temperature stimulus and traverses the discomfort-to-pain regime under conservative stop criteria (Kamper-Fuhrmann et al., 2023; Riley et al., 2010).

In summary, this work asks how adding vibrotactile stimulation to contact heating changes users' multi-dimensional thermal experience, and how such effects can be translated into actionable design choices for wearable and handheld interfaces. We address two research questions:

How vibration parameters—frequency, drive level/amplitude, temporal structure (e.g., duty/pulsing), and stimulation location—affect multi-dimensional subjective outcomes, specifically masking/spread versus tolerability (comfort/acceptability) under controlled warm contact; (RQ1) and Whether a small set of candidate vibration codes (optimized across frequency × amplitude/drive × temporal structure) and placements, selected from RQ1, reliably attenuate thermal unpleasantness during dynamic contact heating relative to a heat-only baseline. (RQ2)

To this end, we conducted a screening study (Experiment 1) to map parameter–percept relationships and select candidates, followed by a ramped-heating study (Experiment 2) with continuous thermal discomfort ratings to quantify window-locked attenuation and derive practical guidance for deploying vibration as a perceptual mitigation strategy.

EXPERIMENTS

This study included two experiments examining whether vibrotactile stimulation modulates thermal discomfort during dynamic heating and whether effects differ by vibration location. Experiment 1 screened candidate vibration codes, and Experiment 2 tested the selected codes under a controlled temperature ramp using continuous slider ratings to analyze window-locked effects against a heat-only baseline.

Participants

Twenty participants (n = 20) were recruited to complete both Experiment 1 and Experiment 2 (within-subject). The participants were all right-handed and reported no known sensory abnormalities or neurological disorders, with intact skin on the upper limb. The age ranged from 20 to 28 years (M = 23.7, SD = 2.25); 9 participants were female and 11 were male. All participants provided written informed consent, and this study was approved by the local institutional review board.

Apparatus

A controlled thermo-vibrotactile system was implemented using a resistive heating pad (300 × 180 × 40 mm) mounted on the prototype surface, as shown in Fig. 1(a). Participants placed the right palm flat on the pad to maintain stable

contact. Surface temperature was monitored at 1 Hz via four thermocouples distributed across the contact area; the four-channel average was used for logging and closed-loop control, while all channels were recorded. Stimulus control and data logging were implemented in a custom Python program interfaced with an Arduino-based controller. Vibrotactile stimulation was delivered by a small ERM motor mounted at three locations (hand-H, wrist-W, forearm-F). Vibration signals were generated by a Rigol DG1032Z waveform generator; across conditions, hardware settings were held constant, and only location and the predefined vibration code/combination varied. Sessions were conducted at 25 °C; participants rested between trials until the tested hand returned to 25 °C and could terminate at any time.

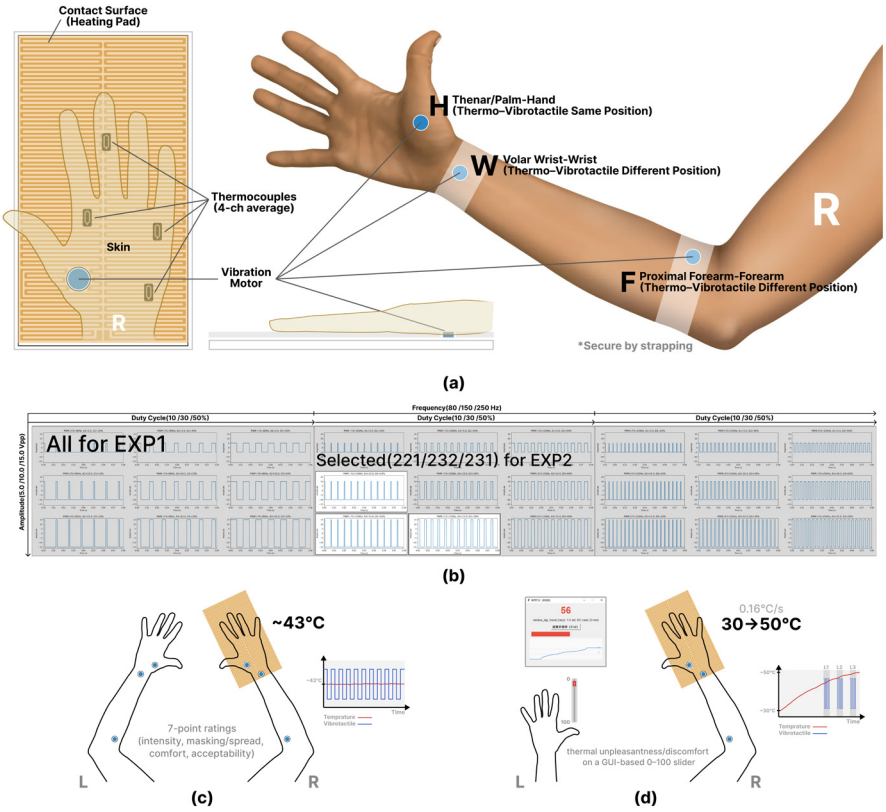

Figure 1: Domains of human system (a) Apparatus overview and three vibration locations (H/W/F) on the upper limb (b) Vibrotactile code set for Experiment 1 and selected codes for Experiment 2 (221/231/232) (c) Experiment 1 screening task (6 position × 27 vibcode): fixed-temperature trials with 7-point multidimensional ratings (d) Experiment 2 validation task (3 position × 3 selected vibcode + 1 Control group): ramped heating with continuous real-time thermal discomfort ratings (baseline vs. vibration).

Procedure

Participants completed two experiments in a within-subject sequence. A brief practice session was provided to ensure that participants could perceive

the stimuli and use the rating interface reliably (i.e., verify compliance and response consistency) before formal trials began. (Jodai et al., 2024) 27 vibration codes were implemented as pulsed (square-wave) carriers with three manipulated parameters (Fig. 1(b)): frequency (80/150/250 Hz), driving amplitude (5/10/15 Vpp), and duty cycle (10/30/50%). The frequency set spans the primary vibrotactile sensitivity band (10–400 Hz) and includes 250 Hz near peak sensitivity (Ng et al., 2020; Rahman et al., 2020; Du et al., 2021); 80 Hz was included as a lower-frequency reference and lies in a range where concurrent warming has been reported to minimally affect vibrotactile thresholds (Singhal et al., 2017). Amplitude was stepped to provide suprathreshold levels for comparison while avoiding overly intense stimulation that may provoke annoyance or startle responses (Chancey et al., 2014). Duty cycle was varied to change the temporal density of vibration (more "tapping"/segmented at low duty cycles vs. more continuous "buzz"-like at high duty cycles), and changes in on–off structure are known to alter perceived vibrotactile quality and intensity (Chancey et al., 2014).

The goal of Experiment 1 was to screen vibrotactile codes/combinations and identify a small candidate set for Experiment 2, as shown in Fig. 1(c). The heating pad temperature was maintained at 42–44 °C via thermocouple-feedback control, a range commonly used to probe local warm discomfort while remaining below typical heat-pain levels for the hand (Zhang et al., 2016, 2017). Vibrotactile stimulation was tested bilaterally at three locations (thenar eminence/hand, volar wrist, proximal volar forearm; six sites total) while code/combination varied across trials. Each trial consisted of a single 3-s stimulation presentation, and each condition was presented at least twice per participant, with randomized order and rest intervals to reduce adaptation (Zhang et al., 2017). After each trial, participants completed four 7-point ratings (intensity, masking/spread, comfort, acceptability). Mean ratings were used to select a strong-effect set (highest masking/spread) and a balanced set (high masking with favourable comfort/acceptability); correlations among dimensions were examined to flag weakly related descriptors as auxiliary.

In Experiment 2, selected candidate codes were evaluated during a dynamic temperature ramp to quantify time-resolved, window-locked effects relative to a heat-only baseline, as shown in Fig. 1(d). Surface temperature was ramped from 30 °C at 0.16 °C/s with a 50 °C safety cutoff (Kamper-Fuhrmann et al., 2023). At session start, participants completed a calibration ramp and used button presses to mark three individualized reference temperatures (thermal discomfort onset, heat pain onset, heat tolerance), which were used to define the three stimulation windows to account for inter-individual variability in thermal responses on the upper limb (Zhang et al., 2016). In the main trials, participants continuously rated thermal discomfort on a GUI-based 0–100 slider (sampled at 1 Hz) logged with temperature and vibration state, enabling fine-grained tracking of small perceptual changes during the ramp (Zhang et al., 2017; Boormans et al., 2009). Heat-only baseline ramps were recorded first, followed by vibration trials in which vibration (from Experiment 1) was delivered at a specified location (H/W/F) within the three individualized windows

(starting 0.5 °C before each reference temperature, lasting 3 s) for window-locked comparisons against baseline.

RESULT ANALYSIS

Experiment 1

Rating structure. Across all codes and sites, ratings showed two coupled pairs: intensity strongly covaried with masking/spread ($r = 0.94$), and comfort covaried with acceptance ($r = 0.88$). Higher intensity was associated with lower comfort ($r = -0.48$) and acceptance ($r = -0.33$). We therefore treated masking/spread as the primary efficacy outcome, with comfort/acceptance as tolerability constraints.

Waveform drivers. Repeated-measures ANOVA indicated that amplitude and duty cycle dominated perceptual outcomes. For intensity, both factors produced large effects at all six sites (Amplitude: $\eta\_g^2 \approx 0.43–0.75$, $p < .001$; Duty: $\eta\_g^2 \approx 0.66–0.84$, $p < .001$). The same pattern held for masking/spread (Duty: $\eta\_g^2 \approx 0.23–0.73$, $p < .001$; Amplitude: $\eta\_g^2 \approx 0.11–0.33$, $p < .001$). In contrast, frequency had negligible influence on most dimensions (typically $\eta\_g^2 \leq 0.02$; intensity up to ≈ 0.04), with only isolated small effects, as shown in Fig. 2(a).

Efficacy–tolerability trade-off. Comfort and acceptance showed smaller but systematic amplitude-related reductions ($\eta\_g^2 \approx 0.16–0.32$), whereas duty cycle contributed little to acceptance and only small, site-dependent changes in comfort (up to $\eta\_g^2 \approx 0.08$).

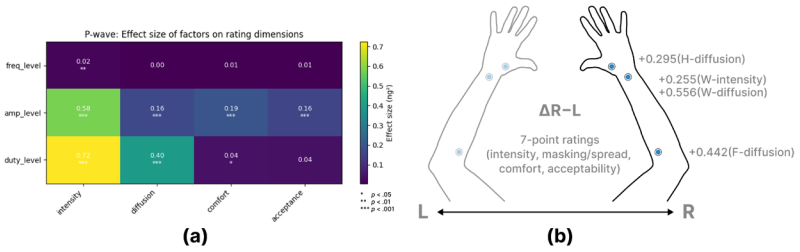

Figure 2: (a) Effect sizes (η_g^2) of frequency, amplitude, and duty cycle on the four rating dimensions(asterisks: * $p < .05$, ** $p < .01$, *** $p < .001$). (b) Bilateral (R–L) differences in ratings across stimulation sites.

Side/location consistency. Bilateral ratings were largely comparable, with only a small rightward bias at the wrist (ΔR–L ≈ 0.25 for intensity; ≈ 0.54 for masking/spread), while the palm/thenar site was near-symmetric, as shown in Fig. 2(b). Location effects were dimension-specific: masking/spread was strongest at the wrist and weakest at the forearm, and tolerability (comfort/acceptance) was generally highest at the wrist and lowest at the hand. Despite these level shifts, code ranking and the masking–comfort trade-off were preserved across sites, supporting generalization across placement.

Candidate Code Selection for Experiment 2

Experiment 1 suggests that amplitude and duty cycle are the primary controllable determinants of perceived efficacy (intensity and masking/spread), whereas frequency is a comparatively low-impact factor within the tested range. The results also demonstrate a consistent efficacy-tolerability trade-off, motivating a graded candidate set rather than a single "best" waveform. Accordingly, we fixed frequency at level2 (150 Hz) to reduce the factorial space and retained three codes that provide a graded coverage of the efficacy-tolerability trade-off, including both a strong-effect and a balanced candidate, as shown in Fig. 1(b):

231 (150 Hz, 15 Vpp, 10%): maximal-efficacy condition (masking/spread ≈ 4.85, intensity ≈ 3.72) with reduced tolerability (comfort ≈ 3.49, acceptance ≈ 3.56).

232 (150 Hz, 15 Vpp, 30%): balanced condition retaining robust efficacy (masking/spread ≈ 4.35, intensity ≈ 3.17) with improved tolerability (comfort ≈ 4.12, acceptance ≈ 4.14).

221 (150 Hz, 10 Vpp, 10%): moderate reference within the same carrier band (masking/spread ≈ 4.31, intensity ≈ 3.08) with comparatively favourable tolerability (comfort ≈ 4.29, acceptance ≈ 4.36).

Finally, given the overall cross-side similarity and the preserved code ranking across hand/wrist/forearm, we simplified Experiment 2 by restricting stimulation to the right hand only, reducing design complexity while maintaining generalizability across placement.

Experiment 2

Analysis interval and window definition. All analyses were restricted to 35–48 °C for two pragmatic reasons: (i) below ~35 °C continuous thermal discomfort ratings were near floor with minimal between-condition separation, and (ii) above ~48 °C attrition increased because some trials terminated early due to discomfort, yielding sparse and non-comparable samples across conditions. We therefore analyzed a common interval and computed windowed metrics using the same temperature binning and window definition across participants.

Three individualized reference windows (L1–L3) were defined from each participant's calibration thresholds. For group visualization, mean thresholds were used to mark window bands (L1 = 42.54 °C, L2 = 45.54 °C, L3 = 48.13 °C).

Results: Group curves and windowed ΔAUC (Area Under Curve). Figure 3–4 show group mean temperature–score curves (35–48 °C) with 95% confidence bands. Across conditions, experimental curves tended to lie below the heat-only baseline, indicating reduced thermal discomfort under vibration. To quantify window-locked effects, we computed ΔAUC within each window band:

$$\Delta AUC = \int_{T \in \text{window}} \left(Score_{\text{cond}} - Score_{\text{base}} \right) dT$$

where negative ΔAUC indicates lower thermal discomfort relative to baseline (i.e., attenuation/masking).

Position effects (Fig. 3). Window L1 showed no reliable position effect (Friedman $p = 0.6065$) and no consistent deviation from baseline across positions. In L2, position differences were significant (Friedman $\chi^2 = 7.87$, $p = 0.0195$). Forearm vibration produced a robust reduction relative to baseline (Wilcoxon $p = 0.0054$, $dz \approx -0.73$), whereas hand and wrist did not reach significance ($p = 0.071$ and $p = 0.160$). Above ≈ 47.35 °C, observations were sparse (approximately n = 8 per position) because conservative stop criteria prioritized participant safety; thus L3 was not used for confirmatory inference. Any remaining negative trend (e.g., forearm) should be treated as exploratory and verified with improved high-window coverage.

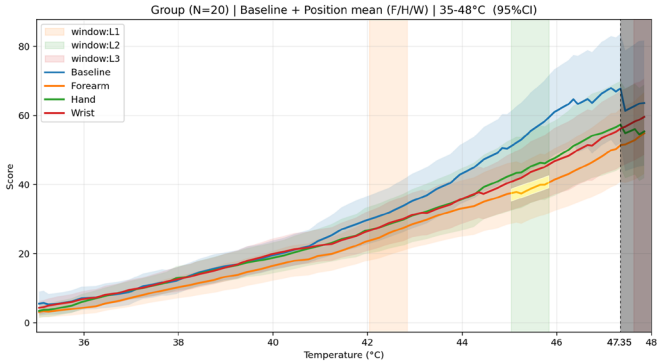

Figure 3: Group mean temperature–score curves by vibration position (35–48 °C). Baseline and position curves (Forearm/Hand/Wrist) show mean thermal discomfort vs. temperature (N = 20; equal weighting); ribbons are 95% CIs.

Vibration code effects (Fig. 4). Across all three windows, there was no reliable separation among vib codes 221/231/232 (Friedman: L1 $p = 0.550$, L2 $p = 0.112$, L3 $p = 0.135$). Nevertheless, within L2, some codes showed significant reductions relative to baseline (221: $p = 0.015$, $dz \approx -0.53$; 232: $p = 0.031$, $dz \approx -0.48$), whereas 231 did not ($p = 0.53$). Thus, code-specific attenuation was detectable for some codes in L2, but overall code ranking was not stable at the group level.

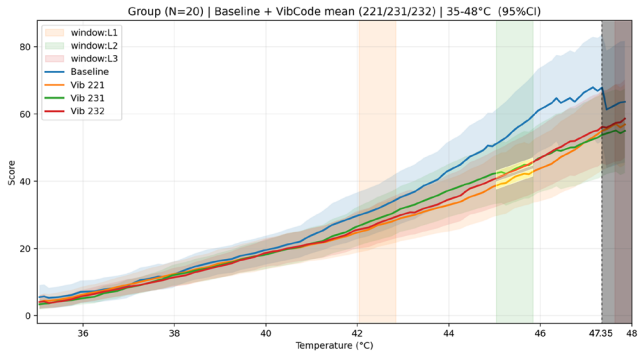

Figure 4: Group mean temperature-score curves by vibration code (35–48 °C). Mean thermal discomfort curves (N = 20) are plotted for baseline and vib codes (221/231/232; equal weighting per participant; averaged across locations as applicable), with 95% CI ribbons.

DISCUSSION

Responses to RQs

Experiment 1 showed a clear structure in subjective outcomes: masking/spread tracked intensity closely, while comfort tracked acceptance, revealing an efficacy–tolerability trade-off. Repeated-measures analyses indicated that amplitude and duty cycle were the dominant drivers of perceived intensity and masking/spread across sites, whereas frequency contributed minimally within the tested range. These patterns were consistent across locations and largely across sides, supporting the use of masking/spread as the primary efficacy indicator with comfort/acceptance as constraint variables when selecting deployable vibration settings.

In Experiment 2, vibration generally reduced thermal discomfort relative to heat-only baseline within the common analysis range (35–48 °C), indicating a directional benefit rather than exacerbation. The attenuation was most reliable in the mid-to-high discomfort band (L2), and location-based differences were more stable than code-based differences: forearm stimulation produced the most consistent reduction, while candidate codes showed limited group-level separability (although some codes exhibited detectable reductions in L2). Together, the findings suggest that (i) vibrotactile stimulation can serve as a practical perceptual mitigation strategy during contact heating, and (ii) for deployment-oriented optimization, where vibration is applied can be at least as consequential as which code is chosen within a reasonable candidate set—making placement a highly design-actionable lever for improving thermal experience.

Further Implications

Overall directional benefit relative to baseline. Within the common analysis interval (35–48 °C), vibration conditions generally yielded lower thermal discomfort than heat-only baseline, reflected by group curves lying below baseline and predominantly negative windowed ΔAUC values. This pattern suggests that adding vibration tends to attenuate rather than exacerbate thermal discomfort, although the strength of attenuation depended on window band and factor (location vs. vib code).

Why effects concentrated in L2. The clearest effects emerged in L2, likely because this band lies in a regime where ratings are above floor (unlike $<$ 35 °C) while sample coverage remains adequate (unlike $\gtrsim$ 48 °C where early termination increases). Practically, L2 provides the best trade-off between sensitivity to modulation and completeness of observations, making it the most informative band for window-locked comparisons. These results further suggest that the most actionable modulation window may lie near the discomfort-to-pain transition (around the individualized pain reference), where thermal discomfort becomes salient but observations remain sufficiently complete; consequently, this band represents the most design-critical interval for deploying vibration to mitigate heat-related discomfort.

Why forearm vibration appeared most effective. Forearm stimulation produced the most stable attenuation (significant and medium-to-large effect size in L2). One interpretation is that a more proximal placement provides

a less spatially-confounded somatosensory context than stimulating near the thermal contact site, yielding clearer modulation of unpleasantness. However, several non-exclusive mechanisms could also contribute: (i) Mechanical/intensity differences—mounting and coupling vary by site, so an ERM motor may deliver different effective acceleration across locations even under identical drive settings; (ii) Co-located thermo–vibrotactile interference—because the palm/thenar region is the heat-contact site, adding vibration at the same locus may increase sensory competition or integration/"fusion" rather than diffusion/masking, reducing the net perceptual benefit (Yarnitsky et al., 1997; Casale and Hansson, 2022); (iii) Attention/expectation—proximal or less expected stimulation may capture attention differently, shifting the weighting of thermal cues during rating. Future work should directly measure delivered acceleration and standardize coupling to disentangle these accounts.

Relative stability of location vs. code. Within the candidate-code set tested here, location effects were more stable and reproducible than code effects: forearm placement yielded the clearest attenuation in the most informative band (L2), whereas code-dependent attenuation was observable in some windows but the group-level ordering among codes did not remain robust across bands.

Limited separability among vib codes. Despite Experiment 1 motivating a graded set (221/232 more tolerable vs. 231 maximal-effect), Experiment 2 did not show a robust group-level main effect of vib code within windows. Under concurrent heating and short windows, perceptual differences among codes may be small relative to inter-individual variability in thermal response and rating strategy, and smaller than location-driven differences. While some codes showed reductions in L2, code-wise separability should be treated as inconclusive at the current sample size and window definition. If multiple codes yield comparable attenuation, selection should be guided by deployment constraints (e.g., wearable form factor, motion context, and social acceptability) rather than masking efficacy alone. Future work should therefore include additional human-factors endpoints—such as perceived annoyance/disruptiveness, attentional capture, and cognitive load or task interference—to identify the most deployable code.

CONCLUSION

Across two within-subject experiments, this study proved that vibrotactile stimulation can attenuate heat-related thermal discomfort during contact heating. However, the robustness of this benefit depends more on where vibration is delivered than on the specific waveform code among the shortlisted set. In the screening study (Experiment 1), subjective ratings revealed a clear efficacy–tolerability structure: amplitude and duty cycle were the primary drivers of intensity and masking/spread, while stronger settings tended to reduce comfort/acceptance, motivating selection of a graded candidate set under a fixed carrier frequency. In Experiment 2, analyses restricted to 35–48 °C demonstrated predominantly negative windowed ΔAUC relative to heat-only baseline, indicating an overall directional improvement in perceived heat experience. The most reliable and design-relevant modulation

emerged in the mid-to-high discomfort band (L2), near the discomfort-to-pain transition, where forearm vibration produced the most stable attenuation, whereas differences among the three candidate codes were not robust at the group level. Collectively, the results suggest that vibrotactile interventions are most actionable when targeted to the transition into high discomfort (around L2) and optimized primarily via placement, providing a practical strategy for mitigating thermal interference in touch-based device contexts.

ACKNOWLEDGMENT

This research was sponsored by the National Social Science Fund of China Art Project (25BG176), the Research Fund for Humanities and Social Sciences of the Ministry of Education (22YJA760082), the Hunan Provincial Degree and Graduate Teaching Reform Research Project (2023JGYB063), Yuelushan Industrial Innovation Center, Lushan Lab Research Funding, the Fundamental Research Funds for the Central Universities. We would like to express sincere gratitude to participants and reviewers for their valuable input throughout this work.

REFERENCES

Boormans, E.M., Van Kesteren, P.J., Perez, R.S., et al. (2009) "Reliability of a continuous pain score meter: real time pain measurement", Pain Practice, 9(2), pp. 100–104.

Casale, R. and Hansson, P. (2022) "The analgesic effect of localized vibration: a systematic review: Part 1: the neurophysiological basis", European Journal of Physical and Rehabilitation Medicine, 58(2), p. 306.

Chancey, E.T., Brill, J.C., Sitz, A., et al. (2014) "Vibrotactile stimuli parameters on detection reaction times", Proceedings of the Human Factors and Ergonomics Society Annual Meeting. Sage CA: Los Angeles, CA: SAGE Publications, 58(1), pp. 1701–1705.

Cholewiak, R.W. and Collins, A.A. (2003) "Vibrotactile localization on the arm: Effects of place, space, and age", Perception & Psychophysics, 65(7), pp. 1058–1077.

Craig, A.D. and Bushnell, M.C. (1994) "The thermal grill illusion: unmasking the burn of cold pain", Science, 265(5169), pp. 252–255.

Du, J.-Y., Huang, Z.-Q., Chen, D.-Y. and Lei, T.-W. (2021) "Current situation of vibration tactile coding", Chinese Journal of Engineering, 43(9), pp. 1261–1268. doi: 10.13374/j.issn2095-9389.2021.01.12.007.

Green, B.G. (1977) "Localization of thermal sensation: An illusion and synthetic heat", Perception & Psychophysics, 22(4), pp. 331–337.

Green, B.G. (2004) "Temperature perception and nociception", Journal of Neurobiology, 61(1), pp. 13–29.

Jodai, T., Jones, L.A., Terao, M. and Ho, H.-N. (2024) "Perceiving synchrony: Determining thermal-tactile simultaneity windows", IEEE Transactions on Haptics, 17(4), pp. 850–859. doi: 10.1109/TOH.2024.3452102.

Johansson, R.S. and Vallbo, A.B. (1979) "Tactile sensibility in the human hand: relative and absolute densities of four types of mechanoreceptive units in glabrous skin", The Journal of Physiology, 286(1), pp. 283–300.

Kakigi, R. and Shibasaki, H. (1992) "Mechanisms of pain relief by vibration and movement", Journal of Neurology, Neurosurgery & Psychiatry, 55(4), pp. 282–286.
Kamper-Fuhrmann, E., Winkler, A., Hahn, A., et al. (2023) "The Hand-Withdrawal-Method—An Adapted and Simplified Method of Limits for Behavioral Heat Pain Assessment", The Journal of Pain, 24(5), pp. 888–900.
Lundeberg, T. (1984) "Long-term results of vibratory stimulation as a pain relieving measure for chronic pain", Pain, 20(1), pp. 13–23.
Melzack, R. and Wall, P.D. (1965) "Pain mechanisms: A new theory: A gate control system modulates sensory input from the skin before it evokes pain perception and response", Science, 150(3699), pp. 971–979.
Mendell, L.M. (2014) "Constructing and deconstructing the gate theory of pain", Pain, 155(2), pp. 210–216.
Ng, K.K.W., Olausson, C., Vickery, R.M., et al. (2020) "Temporal patterns in electrical nerve stimulation: Burst gap code shapes tactile frequency perception", PLoS One, 15(8), e0237440.
Peiris, R.L., Feng, Y.L., Chan, L., et al. (2019) "Thermalbracelet: Exploring thermal haptic feedback around the wrist", Proceedings of the 2019 CHI Conference on Human Factors in Computing Systems, pp. 1–11.
Rahman, M.S., Barnes, K.A., Crommett, L.E., et al. (2020) "Auditory and tactile frequency representations are co-embedded in modality-defined cortical sensory systems", NeuroImage, 215, 116837.
Riley, J.L. 3rd, King, C.D., Wong, F., et al. (2010) "Lack of endogenous modulation and reduced decay of prolonged heat pain in older adults", Pain, 150(1), pp. 153–160.
Roy, E.A., Hollins, M. and Maixner, W. (2003) "Reduction of TMD pain by high-frequency vibration: a spatial and temporal analysis", Pain, 101(3), pp. 267–274.
Singhal, A. and Jones, L.A. (2017) "Perceptual interactions in thermo-tactile displays", 2017 IEEE World Haptics Conference (WHC). IEEE, pp. 90–95.
Villemure, C. and Bushnell, M.C. (2002) "Cognitive modulation of pain: how do attention and emotion influence pain processing?", Pain, 95(3), pp. 195–199.
Yarnitsky, D., Kunin, M., Brik, R., et al. (1997) "Vibration reduces thermal pain in adjacent dermatomes", Pain, 69(1–2), pp. 75–77.
Zhang, H., Hedge, A. and Guo, B. (2016) "Surface and indoor temperature effects on user thermal responses to holding a simulated tablet computer", Journal of Electronic Packaging, 138(3), 031003.
Zhang, H., Hedge, A. and Cosley, D. (2017) "Thermal sensation, rate of temperature change, and the heat dissipation design for tablet computers", Applied Ergonomics, 62, pp. 197–203.